US Department of Defense

GPS/IMU Development of a High Accuracy Pointing System for Maneuvering Platforms

JOSEPH M. STRUS,
MICHAEL KIRKPATRICK, AND
JAMES W. SINKO
SRI INTERNATIONAL

When it comes to providing attitude or designing a pointing system — say, for controlling an airborne antenna or guiding a ship on maneuvers, GPS can use some help. That's where inertial measurement technology enters the picture. Navigation-grade IMUs can handle the job, but researchers at SRI were challenged to see if a less expensive MEMS design could provide suitable accuracy. Turns out it could.

SRI International (SRI) has recently addressed the requirements of pointing systems for a variety of maneuvering platforms. These platforms include airborne systems (unmanned aerial vehicles, aircraft), land vehicles (tanks, HUMVEES), and marine vessels.

Our primary goal was to obtain 0.1-degree pointing accuracy. To achieve this, we considered several design options. A stand-alone navigation grade inertial measurement unit (IMU) seemed too expensive and heavy but has a clear advantage by being more immune to GPS outages. A magnetic compass–based solution appeared too problematic due to calibration and accuracy issues.

After other design trades were reviewed, we limited the path forward to tactical grade IMUs combined with GPS. Several different IMUs were then evaluated for integration into a flexible software package previously developed at SRI for position and attitude tracking of large parachute pallet loads.

A secondary goal was to establish a truth system to verify pointing accuracy of the developed system. The criteria that we set for the truth system were approximately 0.06 degree for kinematic applications and 0.02 degree for static applications. Moreover, we wanted all biases between the units under test and the truth system to be less than 0.01 degree.

Providing truth at this level of accuracy presents difficulties, however. Optical systems can easily attain this level of accuracy for static tests but are difficult for dynamic tests.

A stand-alone GPS attitude system works well for kinematic tests, but the static accuracy requirement would need too long of a baseline to be portable. Ultimately, a hybrid system was developed using both optical and GPS methods.

The first part of this article presents the component analysis and differences for the MEMS IMU versus the tactical grade unit. Then we discuss the design and architecture for the system and the associated GPS/INS navigation processing software. Next we discuss implementation differences for the various components.

Following those sections, we consider the truth systems developed at SRI. Finally, we discuss the tests performed, truth data analysis methodology, and results.

This SRI initiative has led to the implementation of GPS/IMU systems on a variety of platforms.

Evaluating the IMUs

The mid-range, tactical grade IMU discussed in this article incorporates three fiber-optic gyros. The unit employing MEMS gyros has relatively lower power consumption. **Table 1** shows relevant gyro parameters for the two IMUs used. Terminology for each unit is verbatim from the manufacturer's literature.

Our evaluation methodology established a gyro simulation with a consistent power spectral density (PSD) and Allan variance for each unit under test. To do this, multiple runs of greater than 24 hours were made to perform the Allan variance analysis. Short-term runs of less than an hour were used to establish the turn-on bias.

As the most interesting element at this point is the gyros, we have left out the accelerometer component of the analysis. Moreover, the accelerometer performance of the units is not remarkably different.

Analytical Methodology

We set the units up to run stationary at a more or less constant temperature. The temperature control system in use can be assumed to keep the room temperature within 5 degrees F. The units were set to run over several days. In general, we made no attempt to estimate the absolute bias. As a result, the units were oriented pointing more or less north.

Both units output data at nominally 100 Hz. Test software that sums raw delta velocity and delta theta data over 100 samples was used in the units.

Fiber Optic IMU		MEMS IMU	
Gyro bias stability, °/hr, 1 σ (100 sec correlation time)	0.65	Bias in-run stability, °/hr, 1 σ	10
Random walk, °/√hr	0.15	Angular random walk, °/√hr	0.125
Scale factor accuracy, PPM, 1 σ	100	Scale factor linearity, PPM, 1 σ (input > 11.11°/sec)	450
Drift (bias), °/hr, 1 σ	3.0	Bias repeatability, °/hr, 1 σ	30

TABLE 1. Relevant manufacturers' specifications

The principal method we used to measure gyro stability here is the Allan variance, which has previously been employed to study gyro stability in several applications. The Allan variance is defined in IEEE Standard 647; however, we will present the exact definition/algorithm that we used for the discrete Allan variance.

Let $y = (y_i)_{i=1}^{N}$ be a sequence. For each integer τ, $1 \le \tau \ge [N/4]$, define $K = [N/\tau]$ (where [.] denotes integral part) and define the sequence of cluster means $(z_j)_{j=1}^{K}$ by

$$z_j = \left(\frac{1}{\tau}\right)_{k=(j-1)\tau+1}^{j\tau} \sum y_k .$$

The Allan variance of the sequence y with time step τ is defined by

$$\sigma_y^2(\tau) = \frac{1}{K-1}\sum_{i=1}^{K-1}(z_i - z_{i+1})^2 .$$

For the particular Allan variance examples below, the y's are the summed raw gyro rates mentioned above.

Tactical Grade IMU Analysis

Figure 1 presents a raw time-series plot for one gyro in the fiber-optic IMU. This particular data sample is taken over 60 hours. The data show no long-term drifts of any kind.

Figure 2 shows the Allan variance for all three axes of the fiberoptic gyros. All three gyros are nearly identical from an Allan variance standpoint. Figure 2, in which the data ends at 10,000 seconds, exhibits a slope of –1 and therefore confirms the general impression that the data are mostly uncorrelated noise. (For further discussion of this point, see IEEE Standard 1139 referenced in the Additional Resources section near the end of this article.)

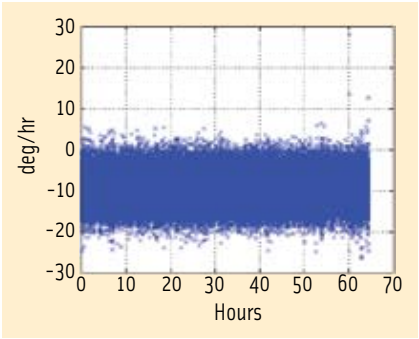

FIGURE 1 Raw fiberoptic IMU data, z gyro

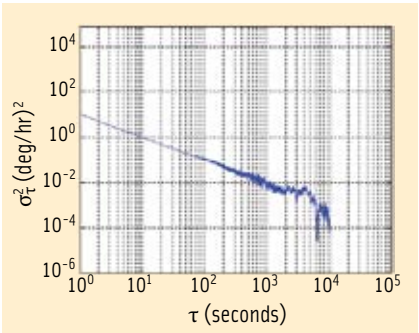

FIGURE 2 Allan variance, fiber-optic IMU z gyro

The nature of the Allan variance curve in Figure 2 suggests that the fiberoptic gyro can be modeled as $K + R(k)$ where K is a constant, R is a time varying term typically referred to as rate noise and k is the sample index of the time process R. The parameters we determined are $K = 7$ (deg/hr)^2 variance and $R = 18$ (deg/hr)^2 variance. Once that is done, a simulation with the predescribed statistics can be generated. The results of the Allan variance of the simulation are in cyan in **Figure 3** and show extremely good agreement with the measured Allan variance.

MEMS IMU Analysis

The MEMS IMU data were collected at the same time and under the same circumstances as the data collection for the tactical-grade fiber-optic IMU. **Figure 4**

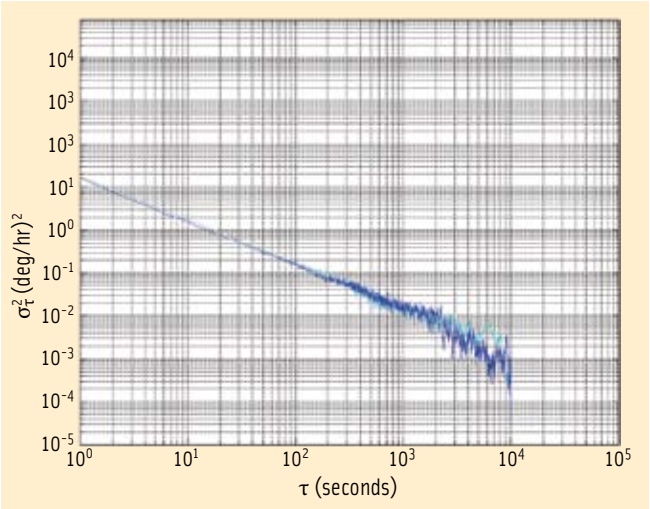

FIGURE 3 Fiberoptic IMU Allan variance, simulated (cyan) and true (blue)

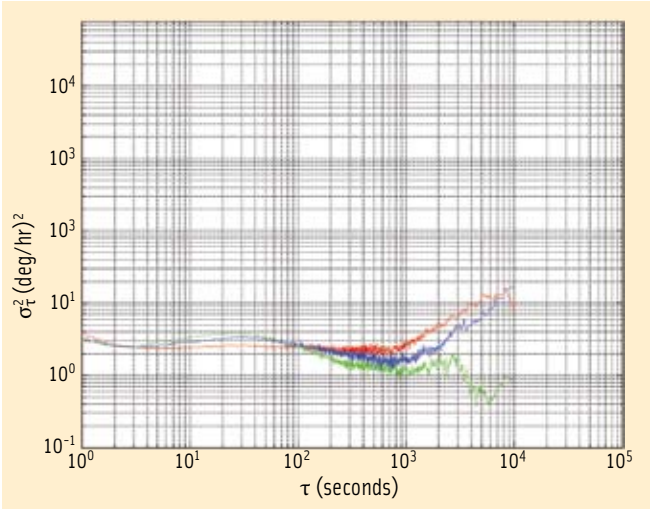

FIGURE 6 MEMS IMU Allan variance all gyros' axes: x, blue; y, red; z, green

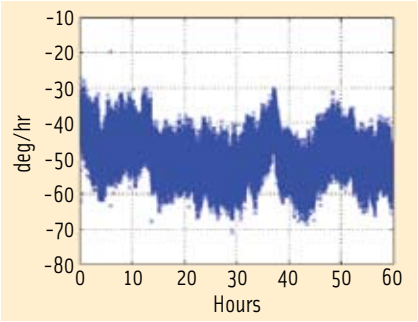

FIGURE 4 Raw MEMS IMU data, z gyro

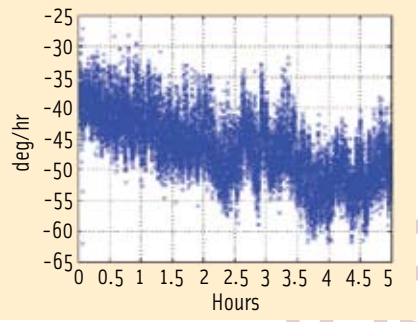

FIGURE 5 Raw MEMS IMU data, z gyro, 5 hours

presents a raw time-series plot for one MEMS IMU gyro.

Figure 5 shows a more detailed plot of only the first five hours of the time series in which an initial rate ramp off seems to appear. However, the same type of behavior occurs at various points in the time series. Therefore, in general, no attempt was made to try to characterize this initial transient.

The Allan variance for the MEMS IMU gyros is presented in **Figure 6**. This chart shows all three axes for one of the sample runs with the x axis data stopped at 10,000 seconds.

Figure 6 initially gives the impression that the curve is nominally flat and, hence, suggests that the dominant noise source is 1/f noise. However, detailed simulation suggests a more complicated picture as will be described later. Nonetheless, the more or less constant slope of the MEMS IMU has important ramifications for the overall system accuracy.

The fact that the Allan variance curve stays generally constant over time suggests that a lower bound of the ability of the end user to estimate the gyro bias is limited to about 1 to 5 degrees per hour. Consequently, a navigation system that reaches such accuracy using Kalman filter techniques should be considered "best possible."

The predominant characteristics of the Allan variance curve are approximately as follows: time 1 to 5 seconds, rate noise; time 5 to 900 seconds, correlated gyro bias; time 900 to 1,000 seconds, flicker floor; time 1,000 to 10,000 seconds, rate random walk.

With these characteristics in mind, a discrete time model for the gyros can be based on the following five terms $r(k) = K + R(k) + C(k) + F(k) + W(k)$ where

- K, constant gyro bias
- R, rate noise
- C, correlated noise
- F, bias instability
- W, rate random walk

where the terminology is the same as in IEEE Standard 647.

We will now show the models for each of these terms with time-varying characteristics.

- R is modeled simply as a Gaussian random sequence, $R(k) = w_R(k)$, where $w_R(k)$ is a real Gaussian sequence with $E(w_R^2) = \sigma_R^2$ and $E(\cdot)$ denotes expectation.
- C is based on the linear Gauss-Markov process $x = -\beta x + \sqrt{2\sigma^2\beta}\,u_C$, where u_C is a normal process with $E(u_C^2) = \sigma_C^2$. The equivalent discrete time realization is given by: $x(k+1) = \alpha x(k) + w_C(k), k = 0,1,2,...$ where $\alpha = e^{-\beta\Delta t}$ is the time constant, and w_C is a normal sequence with variance $\sigma_C^2(1-e^{-2\beta\Delta t})$.
- F is a flicker process and to model it we used the technique described in the article by N. J. Kasdin and T. Walter cited in Additional Resources. We deviate slightly from what the IEEE calls bias instability in that we use a cutoff frequency of 0. The flicker process we model is characterized by 1/f power spectral density and 0 slope on the Allan variance chart.
- The rate random walk term is the limiting case of correlated noise as $\beta \to \infty$ above and is modeled simply as $x = u_w$ where u_w is a normal process with $E(u_w^2) = \sigma_w^2$.

Several minimum variance techniques have been developed to find the coefficients of R, F and W. (See, for

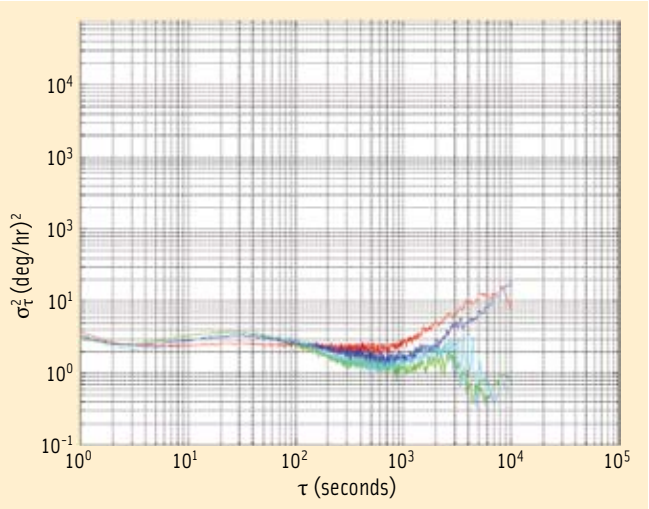

FIGURE 7 MEMS IMU simulated Allan variance (cyan) and three true axes

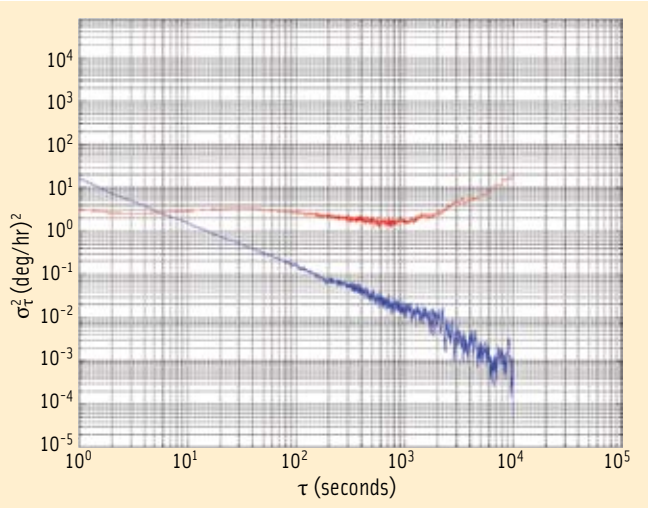

FIGURE 9 Tactical grade fiber-optic (blue) and MEMS IMU (red), Allan variances

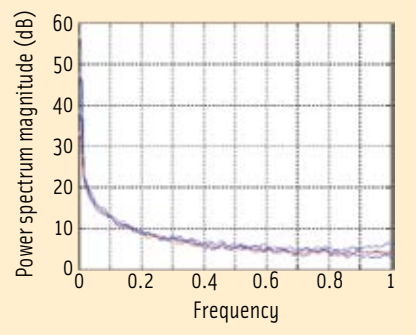

FIGURE 8 MEMS IMU gyro and simulation PSDs.

example, the presentation by F. Vernotte et alia cited in Additional Resources.) These techniques were largely developed for precision oscillators where epoch to epoch correlation is minimal. Due to the presence of the correlated noise term *C*, we resorted to an ad hoc approach to determine the coefficients.

The values found for these individual terms are as follows:

- *R* is Gaussian noise with variance 0.49 (deg/hr)^2.
- *C* has time constant 19.4 seconds and driving noise with variance 0.00392 (deg/hr)^2.
- *F* is simulated as 1/f noise with variance 3.61 (deg/ hr)^2.
- *W* is random walk with driving noise variance 3.82e-4 (deg/hr)^2.

Figure 7 displays the results of an Allan variance simulation of the MEMS IMU performance based on these values. There, the cyan curve is the simulated curve. The agreement is excellent up to 1,000 seconds. After 1,000 seconds, the curve drops off slightly, but this is largely due to this particular instance of the random sequences used to drive the simulation.

To further verify the integrity of the simulation, the power spectral density of the curves was considered. To simplify the analysis, we used the MATLAB function *psd* with the default options. The results are shown in **Figure 8** where the red curve is the psd of the simulated series and the blue curves are from the measured gyros. The values at low frequency do not agree due to the data biases. For ease of comparison, **Figure 9** shows the Allan variance curve of the MEMS IMU and the fiber-optic IMU on the same curve.

GPS/INS Integration

The integrated navigation systems that we tested and describe in this article consisted of tactical grade IMUs coupled with a 17-channel GPS engine augmented by a commercial satellite-based real-time differential correction service and a microcomputer to combine the GPS and IMU data. The overall hardware package length was shrunk for the MEMS IMU.

The units weigh about 10 pounds including battery power adequate for four hours of run time. The units can also output real-time data and accept external DC power for longer run times. An additional feature in the systems is the ability to record raw data for post-processing. This feature allows an additional performance criterion to be estimated. A much more compact package is being developed for a smaller MEMS IMU.

The embedded software has a modular design allowing quick prototyping for different inertial sensors. Data rates and various other real-time parameters are set via external controller/viewer software (**Figure 10**).

In differential GPS (DGPS) mode, the receiver's horizontal accuracy was approximately one meter in good environments, and somewhat worse than that in partially obscured environments. In clear conditions with continuous L1 and L2 tracking, the receiver is capable of using an extra precision mode after a number of minutes. After approximately 10 minutes of continuous operation in the latter mode, the receiver produced horizontal accuracies of about 30 centimeters.

FIGURE 10 Controller/viewer software

For ground tests of the truth system, a van was equipped with a boom on which the IMU/GPS units were mounted. The telescopic scope on the side of the boom was used for sighting distant landmarks used as reference points.

Loss of too many satellite signals — for example, as a result of obstructions or interference — will result in the satellite-based augmentation service going from high-precision to DGPS mode. The return to the high-precision mode can occur within as little as two minutes, although in some cases it is appreciably longer.

The Kalman filter in the real-time software has 15 states, three each for position errors, velocity errors, tilt errors, accelerometer bias, and gyro bias. A more detailed description of the Kalman filter used in integrating the GPS and IMU appears in the article by J. Strus et alia cited in Additional Resources.

Kalman Filter Modifications

The fiber-optic gyros are adequate to perform stationary alignment error estimation by gyrocompassing. This usually results in an initial azimuth error of one to two degrees.

In contrast, the MEMS IMU does not produce a useful gyrocompassing result due to the large turn-on bias. So, we added a motion alignment capability to the latter unit. Moreover, additional compensation algorithms were added for the potentially large initial uncertainties when motion alignment was not desired.

Based on the Allan variance analysis described earlier in this article, proper gyro modeling requires three states for each MEMS IMU gyro. Based on our design constraints, we opted for a state reduction model such as is discussed in the article by R. L. Greenspan (Additional Resources). Gyros are simply modeled as Gauss/Markov processes with a large time constant. This allows us to tune the filter bias uncertainty to a value very close to that predicted by the Allan variance. In our experience, the decrease in complexity is a reasonable compromise.

Truth Systems

We used two different truth systems to verify the accuracy of the units under test. For ground tests, the GPS/INS systems were mounted on a 4.6 meter boom on a minivan. The boom was designed and engineered to precise tolerances in a machine shop and has carefully mounted L1/L2 GPS antennas on each end.

This design allows the system to be tested against a long-baseline GPS attitude system with an estimated accuracy of 0.06 degree in azimuth, and 0.12 degree in pitch for a single measurement. The boom also has a telescopic rifle scope so that distant landmarks can be sighted with an estimated accuracy of 0.015 degree.

The RTK algorithms are described in the articles by J. W. Sinko and C. Basnayake et alia (see Additional Resources). With the two IMU/GPS units mounted in the middle, the boom can be swung in both azimuth and pitch so that it can be aimed at distant landmarks. For static ground tests the boom has a telescopic rifle scope to sight distant landmarks, which can be seen in the accompanying photo. With good GPS positional accuracy (± one meter) of the landmark and the vehicle, and with the landmark being at least 10 kilometers away, the estimated accuracy of the pointing system is 0.015 degree.

Test Results

Figure 11 shows about 100 minutes of data collected on streets and in a parking lot with good sky coverage. It also illustrates a number of performance characteristics of the two different IMU/GPS units under test. The interval from 340,500 to 341,500 seconds traversed about 10 kilometers of city streets and expressways as well as some freeway.

GPS availability ranged from poor to good and only DGPS mode was attained. During this time the Kalman filters in each unit did a reasonable job of estimating the IMU gyro biases.

At 341,940 seconds, the vehicle was stopped and the boom pointed at a landmark with an azimuth of 83.75 degrees. The vehicle remained stationary for about 1,000 seconds. During this time the fiber-optic-based unit drifted very little, while the MEMS IMU–based unit drifted more than a degree — as predicted by the Allan variance tests.

Figure 12 shows how the units performed with respect to the telescopic gun sight, at least until 342,237. At that time, the wind shifted the boom slightly. Another slight wind jump occurred, and then, at 342,600 seconds, the boom was manually set back to the original azimuth.

Again referring to Figure 11, starting at 343,040 seconds after five minutes of driving the IMUs were reasonably well aligned again and little drift was observed over a 1,000-second near-static period starting at 343440. The van was

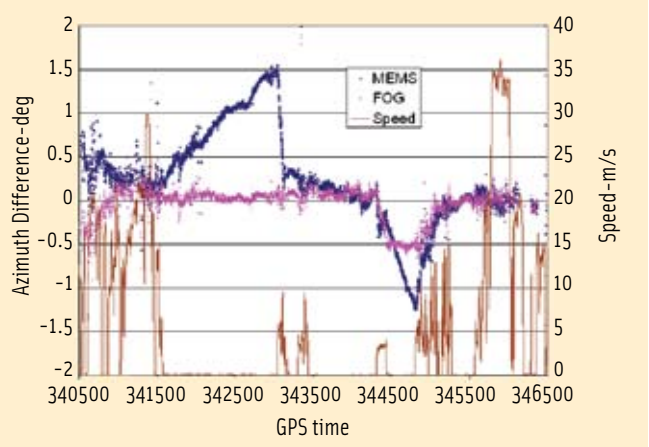

FIGURE 11 A 100-minute test run

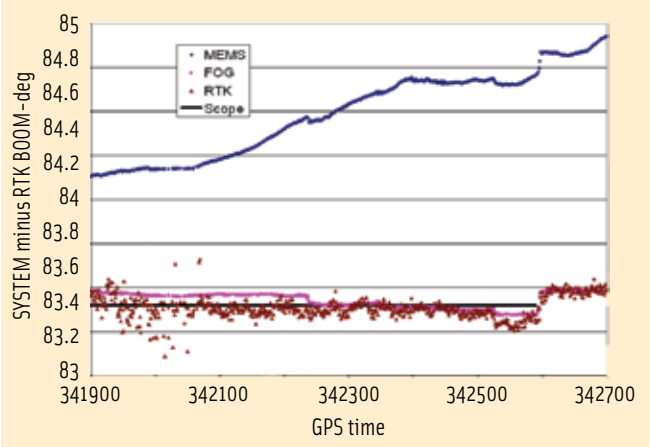

FIGURE 12 Gyro drift while boom was stationary.

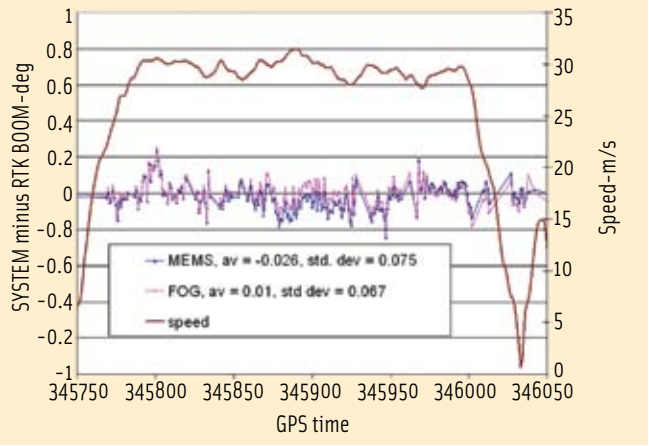

FIGURE 13 Azimuth difference (IMU/GPS–RTK GPS) during a four-minute freeway drive

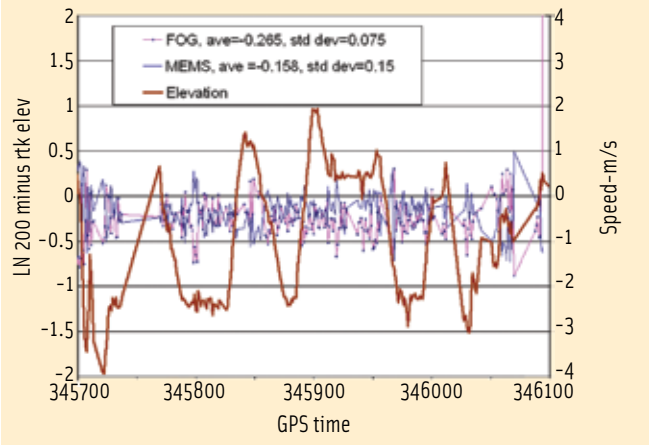

FIGURE 14 Elevation difference (IMU/GPS–RTK GPS) during a four-minute freeway drive.

stationary, but the boom was pointed at several landmarks. The MEMS IMU started a bit off and drifted through the actual azimuth.

Figure 11 details significant gyro runoffs beginning at time 344,350. This was caused by making 10 successive left-hand circles at the minimum turn radius of the minivan. Our interpretation is that this error is due to scale factor error, because the 0.25- to 0.5-degree error is in the realm of what would be expected based on the manufacturer's specifications in Table 1.

After another eight minutes of slow speed driving (less than 10 m/s), a few more static tests were made and then the van was driven on a mostly unobscured freeway for about four minutes. Although the GPS has correlated multipath error when it is stationary, introduction of platform dynamics allow this error to be averaged down.

Extensive testing of a 1.2-meter GPS attitude system indicates that the short-term (minutes) bias error is typically 0.25 degree, and the standard deviation is also about 0.25 degree. When averaged over a sidereal day, the bias dropped to 0.06 degree because the phase multipath was averaged over a large part of the sky.

If the attitude system is moved significantly in azimuth, a similar multipath-averaging effect occurs. Translating these results to the 4.66-meter baseline used in these experiments gives an expected dynamic bias of 0.015 degree with a standard deviation of 0.06 degree.

The averaging technique basically uses the stability of the IMU to average the GPS. Generally, researchers would consider it undesirable to use a unit under test to play a part in determining the accuracy of that unit. However, in this case it makes sense to do just that given the difficulty of measuring azimuth on a moving vehicle.

Figure 13 shows the difference between the GPS azimuth and the IMU azimuths for about four minutes on a suburban freeway. While the difference jumps around by about 0.1 degree on an epoch by epoch basis, averaging over any one minute period reduces the difference to about 0.03 degree.

This approach is affirmed by **Figure 14**, which shows the elevation angles (pitch) measured by the IMUs and the GPS attitude system. In this case, the IMUs are known to be quite accurate —throughout entire runs the two units track each other in elevation within 0.05 degree. The elevation angle given is not very dependent on GPS because the IMUs always have the acceleration of gravity.

On the other hand, the GPS attitude system will have an elevation error of

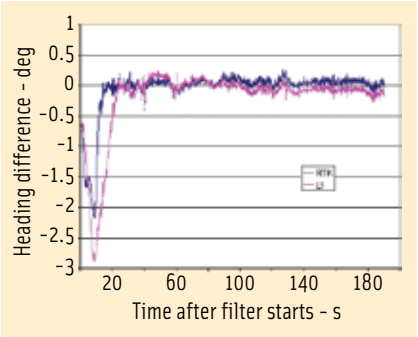

FIGURE 15 Azimuth difference using RTK and L1 only GPS with a moving start

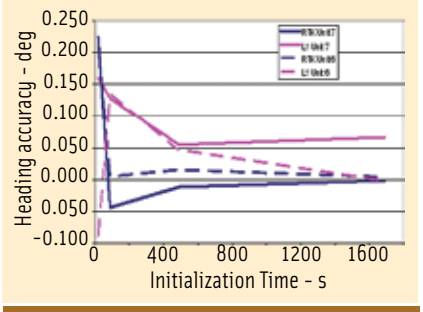

FIGURE 16 Heading accuracy versus initialization time

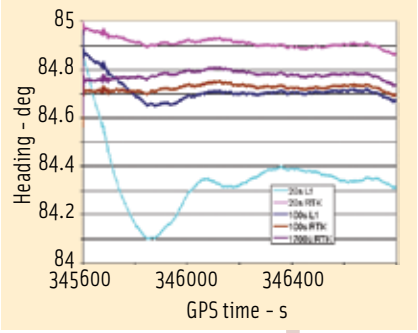

FIGURE 17 Heading values of different configurations after initialization

about twice the azimuth error (or about 0.12 degree) because of the unfavorable DOP (dilution of precision) associated with elevation measurements. Again the average works out to a constant offset (while the IMUs were carefully mounted in azimuth, they were not carefully mounted in pitch).

Rapid turn rates also introduced an error apparently due to residual scale factor error. At low speeds the attitude accuracy depended on the accuracy of the GPS measurements, but at aircraft speeds C/A-code GPS produced attitude accuracies as good as RTK GPS measurements.

We performed a final series of tests to determine the quality of GPS data necessary for accurate azimuth alignment. Two Autonomous Inertial Reference System (AIRS) units with fiber-optic IMUs were used for the tests. The tests took place in the clear when both L1 GPS and GPS RTK positioning was available. To obtain these solutions, commercial L1/L2 receivers were used.

Figure 15 shows the filter convergence during a moving start. The figure shows the difference between the Kalman filter solution for heading and the heading determined by the 4.6-meter baseline GPS attitude system on the boom. When fed RTK data the filter converges a bit faster with a slightly lower maximum error than when the filter is fed L1 data. As the GPS attitude system is only accurate to about 0.1 degrees, not many conclusions can be drawn after 30 seconds.

Figure 16 shows the Kalman filter accuracy as determined by the telescopic rifle sight, which has an estimated accuracy of 0.01 to 0.02 degrees. Data is shown for several initialization periods. All initialization was done while moving at relatively slow velocities (2 to 15 m/s). A three-minute delay occurred between stopping and having the boom lined up to make the measurement.

Again, the RTK data usually does a better job of aligning the filter. Accuracy is quite high after 100 seconds of alignment with RTK data. A longer alignment time helps when only L1 data is available.

We should note that this data was for a single run of one AIRS unit and that somewhat different numbers will occur for other runs. However, these results are representative.

Figure 17 reveals the drift of the units after different alignment data sets. The data shown are for a 1,200-second period with the boom locked down. The period starts about four minutes after the vehicle stopped. With only 20 seconds of moving alignment, drift occurs in both the L1- and RTK-aligned units, but the drift is much more severe for the L1 case.

Even after 100 seconds the L1 case shows some drift while the RTK case is quite stable, but with about 0.05 degrees in error. For alignment periods of 500 seconds or more, both the L1 and RTK cases produce high stability, although as shown in Figure 17 the accuracy of the RTK alignment is generally better.

Conclusions

With suitable dynamics, both varieties (fiber-optic and MEMS) of IMU/GPS combinations were capable of providing an azimuth to within at least 0.06° 1 σ. Furthermore, the Allan variance analysis accurately predicted the azimuth drift performance of the IMU systems.

Additional testing on the FOG units showed azimuth to be determined faster and more accurately with RTK data than with L1 data. The telescopic sight proved to be a convenient way of testing for static cases. The long-boom GPS attitude system, coupled with averaging, appears to give very good testing accuracy during dynamics.

At low speeds the attitude accuracy depended on the accuracy of the GPS measurements, but at aircraft speeds C/A-code GPS produced attitude accuracies as good as RTK GPS measurements.

Acknowledgment

We wish to thank Patrick Weldon of Honeywell for lending us on short notice the MEMS unit used in our tests.

Additional Resources

Basnayake, C., and C. C. Kellum, J. Sinko, and J. Strus, "GPS-Based Relative Positioning Test Platform for Automotive Active Safety Systems," ION GNSS 2006, pp. 1457–1467

Brown, R. G., and P. Y. C. Hwang, *Introduction to Random Signals and Applied Kalman Filtering*, John Wiley & Sons, New York City, USA, 1992

Greenspan, R. L., "GPS and Inertial Integration," in *Global Positioning System: Theory and Applications Vol. II,* pp. 187–220, (Edited by B. W. Parkinson and J. J. Spilker), American Institute of Aeronautics and Astronautics, Washington, D.C., 1996

"Honeywell User's Manual for HG1900BA99," Minneapolis, Minnesota USA, 2004

Hou, H., "Modeling Inertial Sensors Errors Using Allan Variance," Masters Thesis, University of Calgary, Geomatics Engineering, UCGE Report 20201

IEEE Std 647–1995 Annex C: IEEE Standard Specification Format Guide and Test Procedure for Single-Axis Laser Gyros—An Overview of the Allan Variance Method of IFOG Noise Analysis

IEEE Std 1139–1999 IEEE Standard Definitions of Physical Quantities for Fundamental Frequency and Time Metrology—Random Instabilities

Kasdin, N. J., and T. Walter, "Discrete Simulation of Power Law Noise," 1992 IEEE Frequency Control Symposium, pp. 274–283, 1992

Litton LN-200 Inertial Navigation Measurement Unit, Source Control Document, Woodland Hills, California USA, 2000

Sinko, J. W., "RTK Performance in Highway and Racetrack Experiments, *Navigation*, Vol. 50, No. 4, pp 265–275, 2003

Strus, J. M., and E. G. Blackwell, C. A. Gellrich, M. R. Kirkpatrick, J. W. Sinko, "Instrumentation of Paratroopers and Large Pallet Loads," ION GPS 2002, pp 2457–2465, 2002

Van Dierendonck, A.J., and J.B. McGraw, and R.G. Brown, "Relationship between Allan variances and Kalman filter parameters," *Proceedings of the 16th Annual Precise Time and Time Interval (PTTI) Applications and Planning Meeting,* NASA Goddard Space Flight Center, pp 273–293, Accession Number 85N29238, 1984

Vernotte, F., and E. Lantz, J. Groslambert, and J. J. Gagnepain, "A New Multi-Variance Method for the Oscillator Noise Analysis," 1992 IEEE Frequency Control Symposium, pp 284–288

HG1900 package

LN-200 package

Manufacturers

The fiber-optic tactical grade IMU described in this article was the A=2 model of the Litton LN-200 (311875-240207) manufactured by **Northrop Grumman,** Woodland Hills, California, USA. The MEMS IMU was the HG1900 BA99 by **Honeywell Aerospace Electronic Systems,** Minneapolis, Minnesota, USA. The INS systems incorporated an OEMV receiver from **NovAtel, Inc.,** Calgary, Alberta, Canada, using the **OmniSTAR** satellite-based augmentation service, Houston, Texas, running in the VBS/XP modes.

Authors

Joseph M. Strus <joseph.strus@sri.com> is a systems analyst at SRI International, Menlo Park, California, where he has worked on precision navigation applications since 2001. His interests are GPS, GPS/INS, and estimation theory. Previously, he was a GPS systems engineer with the Government Systems Division of Rockwell Collins. Strus received his B.S. and Ph.D. (mathematics) from the University of Illinois at Urbana-Champaign and holds several GPS-related patents.

Michael Kirkpatrick <michael.kirkpatrick@sri.com>is currently a senior research engineer at SRI International, where he has been involved in hardware and software systems design and development since 1985.

James W. Sinko is a principal engineer at SRI International. He received his B.S. (engineering science) and M.S.E.E. from Stanford University, and his Ph.D. (E.E.) from the University of Rochester. Sinko has been with SRI since 1967, working with radar and aircraft systems. For the last 13 years, he has been working with precision GPS for military and civil applications.